Quaternary Science Reviews 122 (2015) 63–73

Contents lists available at ScienceDirect

Quaternary Science Reviews

journal homepage: www.elsevier.com/locate/quascirev

Lake Qinghai sediment geochemistry linked to hydroclimate variability since the last glacial

Zhangdong Jin [a, b, *], Zhisheng An [a, b], Jimin Yu [c], Fuchun Li [d], Fei Zhang [a]

[a] State Key Laboratory of Loess and Quaternary Geology, Institute of Earth Environment, Chinese Academy of Sciences, Xi'an 710075, China
[b] Institute of Global Environmental Change, Xi'an Jiaotong University, Xi'an 710049, China
[c] Research School of Earth Sciences, The Australian National University, Canberra, ACT 0200, Australia
[d] College Resources and Environmental Science, Nanjing Agricultural University, Nanjing 210095, China

ARTICLE INFO

Article history:
Received 28 September 2014
Received in revised form
16 April 2015
Accepted 13 May 2015
Available online 7 June 2015

Keywords:
Sediment geochemistry
Lacustrine precipitate
Hydroclimate
Ca^{2+}-limited lake water
Asian dust
Lake Qinghai

ABSTRACT

Geochemistry of basin sediments from semi-arid regions is valuable to understand past hydroclimatic changes. Here, we investigate the links of sedimentary geochemistry (Rb, Sr, Ca/Zr, TOC, and %$CaCO_3$), carbonate mineralogy and ostracod shell $\delta^{18}O$ of Lake Qinghai, a basin proximal to major dust production centers at mid-latitudes of the Northern Hemisphere, to changes in depositional conditions and hydroclimate during the past 32 ka. Surface lacustrine sediments are characterized by low-Rb, high-Sr, low-Rb/Sr, high-%$CaCO_3$ and high-Ca/Zr values, in contrast to the chemical compositions of eolian loess (high-Rb, low-Sr, high-Rb/Sr, low-%$CaCO_3$, and low-Ca/Zr). A direct comparison of soluble Ca and Sr in two short cores with instrumental water discharge data suggests that lacustrine precipitates in Lake Qinghai are dominated by authigenic aragonite formed under Ca^{2+}-limited water conditions, and that the accumulation rate of aragonite dominantly depends on solute fluxes into the lake during the rainy seasons (late May to September). Our high-resolution down-core records show that sediments during the last glacial (~32–19.8 ka) had high-Rb, low-Sr, low-%$CaCO_3$, and low-Ca/Zr, indicating eolian dust (loess) accumulation in a desiccated basin under dry glacial conditions, further supported by grain size and pollen results. This type of sedimentation was maintained during the last deglacial (~19.8–11.5 ka), but interrupted by episodic lacustrine precipitates with high-Sr, high-%$CaCO_3$, high-Ca/Zr, and low-Rb. At ~11.5 ka, sedimentary Rb/Sr, Ca/Zr, %$CaCO_3$ and TOC show dramatic and permanent changes, implying an abrupt shift in the atmospheric circulation at the onset of the Holocene in the Lake Qinghai region. Lacustrine precipitates have persisted throughout the Holocene with a maximum during the early to mid-Holocene (~10.5–8.0 ka). Since ~8.0 ka, the gradual and significant decreases in aragonite and Sr accumulations in tandem with increasing dust deposit and more positive ostracod $\delta^{18}O$ may be linked to a weakening of Asian summer monsoons during the mid-to-late Holocene. Overall, our records appear to show a high sensitivity of sediment development and geochemistry in Lake Qinghai to the regional hydroclimate changes since the last glacial.

1. Introduction

Dust deposition plays a significant role in transporting exogenous materials to lacustrine sediments, in particular to lake systems located at mid-latitudes of the northern hemisphere (e.g. Andreae, 1996; Dean, 1997; Lawrence and Neff, 2009; Wan et al., 2012). When dust compositions remain stable and are different from those of the catchment, changes in dust fluxes of various provenances should affect lake sediment chemistry (e.g. Guerzoni et al., 1999; Ganor et al., 2003; Jin et al., 2009; Mulitza et al., 2010). Determining compositions of dust and temporary changes in the dust fluxes to the basin of interest is essential (1) to understand sediment chemistry, (2) to extract information contained in the sediments, and (3) to reconstruct the paleoenvironment from various proxies of sediments. Therefore, down-core lacustrine sediment geochemistry may be used to infer variations of dust budget in the past, which could be potentially linked to the regional environmental history. This study aims to investigate a suite of

* Corresponding author. State Key Laboratory of Loess and Quaternary Geology, Institute of Earth Environment, Chinese Academy of Sciences, Xi'an 710075, China.
E-mail address: zhdjin@ieecas.cn (Z. Jin).

http://dx.doi.org/10.1016/j.quascirev.2015.05.015
0277-3791/

sedimentary geochemistry tracers in Lake Qinghai and their responses to hydroclimate changes during the last 32 ka.

Owing to its unique geological and climatic settings (Fig. 1a), Lake Qinghai has attracted many studies for paleoclimatic and ecosystem reconstructions (e.g. Lister et al., 1991; Shen et al., 2005; Ji et al., 2005; An et al., 2012; Fu et al., 2013; Liu et al., 2014; Thomas et al., 2014), and is one of most intensively investigated lake systems (see the reviews by Colman et al. (2007) and Henderson and Holmes (2009)). Previous studies have provided valuable information about climate changes and their responses to the interplay between the northern Westerlies and Eastern Asian or Indian summer monsoons during the last 16 ka. For example, measurements of pollen, total organic carbon (TOC), grain size, carbonate content (%$CaCO_3$) and ostracod shell stable isotopes for sediment cores QH85-14 (e.g. Kelts et al., 1989; Lister et al., 1991) and QH2000 (Liu et al., 2003; Shen et al., 2005) suggested a warming in Lake Qinghai starting around 14.5 ka (corresponding to Bølling warming in Greenland), followed by a brief cold reversal. These studies showed that the maximum warming occurred at ~10.0 ka, and remained warmer than the present until ~4.0 ka. Based on grain size, TOC and %$CaCO_3$ proxies from core 1Fs, An et al. (2012) suggested a dry condition predominantly controlled by the northern Westerlies during the Last Glacial Maximum (LGM) with greater westerly influence, and much wetter conditions during the early Holocene which was attributed to a greater influence of the Indian and Eastern Asian summer monsoons. Despite these efforts invested so far, past hydrological and depositional conditions of Lake Qinghai remain poorly constrained, limiting our understanding of sediment proxies and their hydroclimatic implications.

Because of the amplification effect at high elevations (Liu et al., 2009; Diffenbaugh et al., 2012), Lake Qinghai, located at ~3200 m above sea level (m a.s.l.), is particularly sensitive to hydroclimate changes. Today, hydroclimate at Lake Qinghai is mainly affected by the convergence of the northern Westerlies and monsoonal-dominated climate regimes (Fig. 1a). Another advantage is that the hydrologically-closed drainage is minimally disturbed by anthropogenic activities, making the sediments in this lake ideal to investigate geochemistry changes in response to natural processes including moisture sources to the lake and hydroclimate changes affecting the region (Fig. 1b).

As a huge water body located at the midpoint of the modern “airborne dust corridor” (Fig. 1a) (Liu et al., 2008), Lake Qinghai receives materials from catchment weathering and airborne dust inputs, both of which are closely linked to hydroclimatic conditions. A significant contribution of dust to modern Lake Qinghai is strongly supported by modeling (Jin et al., 2009) and field measurements of seasonal river water chemistry (Jin et al., 2011) and eolian dust (Wan et al., 2012). Furthermore, yellow–brown sediments at some periods in core 14B in Lake Qinghai have been described as underwater loess deposition (Lister et al., 1991). Sediments of eolian origin have also been supported by more recent works on color, grain size and morphology of sediments (An et al., 2012; Fu et al., 2013). Detailed knowledge of relative contributions of dust to Lake Qinghai is crucial for understanding (1) impacts of mineral aerosols on sediment properties, (2) proxy implications for hydroclimatic conditions, and (3) interactions between the Indian and East Asian summer monsoons and the Westerlies in the past. However, we have limited information about the flux and geochemistry of dust into Lake Qinghai, limiting our understanding of the relationship between dust deposition and hydroclimate changes in the past. We fill in this critical gap in this study.

An 18.3 m long high-resolution sediment core (1Fs) provides a unique opportunity to gain insight into dust contributions to Lake Qinghai during last glacial-interglacial cycle. This work builds on previous work by An et al. (2012) who developed an age model (cf. Zhou et al., 2014) and initial climatic reconstruction from the 1Fs. In order to identify relative contributions of eolian dust versus lacustrine precipitates to Lake Qinghai sediments under different depositional and hydroclimatic conditions, we have focused on a few geochemical tracers including Rb, Sr, and Ca/Zr for recent lake and river sediments and catchment loess, and for sediments from the core 1Fs. In the context of existing sedimentological and biological records, we then discuss changes of dust input and lacustrine precipitates in relation to the regional hydroclimate dynamics since the last glacial.

2. Hydrological and geological settings of the Lake Qinghai catchment

Lake Qinghai has been a hydrologically closed drainage system since ~36 ka (Chen et al., 1990). During the last century, the surface area of the lake shrank from 4980 km^2 to ~4260 km^2 in 2006 (Li et al., 2007). The modern lake is located at an altitude of 3194 m a.s.l., with a water volume of 71.6 km^3 and a catchment area of about 29,660 km^2. Today's lake water has an average salinity of 15.5 g/L and pH of 9.06. Currently, the lake is Ca^{2+}-limited and is saturated with respect to carbonates. Lake sediment is dominated by silty clays and authigenic carbonates (aragonite and calcite).

The lake is currently fed by five major rivers including Buha, Shaliu, Hargai, Quanji, and Heima Rivers (Fig. 1b), with a total annul water discharge of ~1.56×10^9 m^3 (Li et al., 2007). The main runoff supply today is from the Buha River from the west, which feeds annually ~50% of the total runoff and ~70% of the total sand loading to the lake. The average annual water discharge was ~0.94×10^9 m^3 in 1959–2013 at the Buha Hydrology Station, with ~85% occurring during monsoon season (late May to September). By comparison, the annual water discharge of the Shaliu River at Gangcha County is about one third of discharge from the Buha River.

Within the Lake Qinghai catchment, the average annual air temperature was ~1.2 °C from 1951 to 2005. The annual mean precipitation was 383 mm, about 1/4–1/3 of the evaporation, during 1959–2011 (Jin et al., 2011). The lake develops a thermal stratification (hypolimnion <6 °C, epilimnion 12–15 °C) during summer, and is frozen from late October to April (Yan et al., 2002).

The Lake Qinghai catchment comprises of hummocky terrains of predominantly late Paleozoic marine limestone and sandstones, Triassic granites, Mesozoic diorite and granodiorite with minor late Cambrian phyllite and gneiss (LIGCAS, 1979). About one fifth of the catchment is overlain by Quaternary to recent loess and alluvial/lacustrine sediments surrounding the lake and its contributing rivers.

3. Samples and analyses

3.1. Surface sediment and loess samples

We collected 17 surface lake sediments, 24 local loess, and 25 suspended sediment samples from five largest rivers within the Lake Qinghai catchment. Suspended sediments were sampled by passing water during monsoon seasons through 0.2 μm nylon filters. Samples of fresh loess and lake surface sediment were collected from extensive sites within the catchment (Fig. 1b).

3.2. Core sediments and age models

The 18.3-m-long 1Fs core was composited the cores 1F with 1A based on the correlations of lithological and proxy data (An et al., 2012). Both 1F and 1A were retrieved from the same site at the deposition-center (36°48′40.7″N, 100°08′13.5″E, 3194 m a.s.l.) of the southwestern sub-basin in Lake Qinghai in 2005 using the ICDP

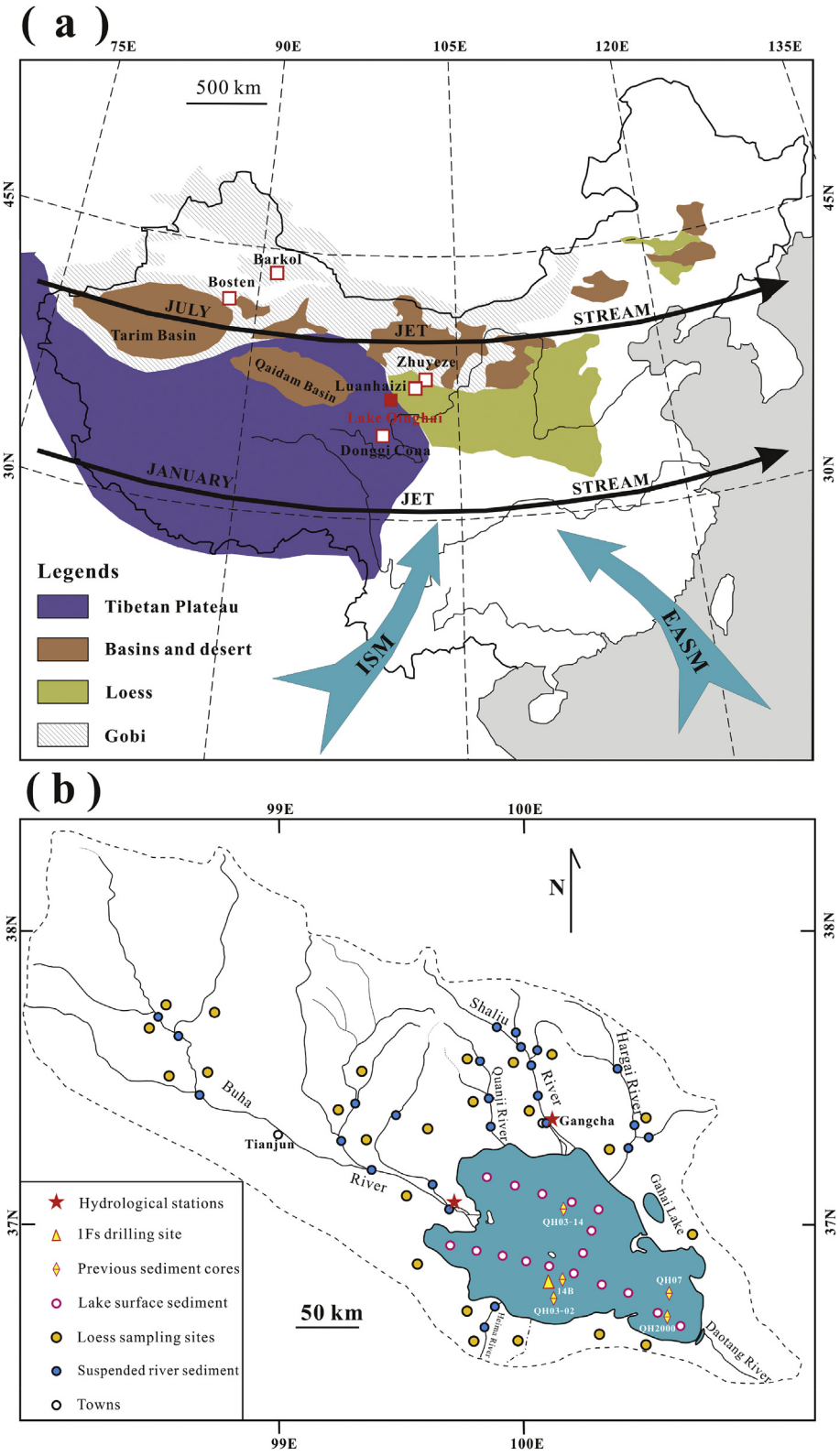

Fig. 1. (a) Geological and climatological locations of Lake Qinghai, and other lakes mentioned in the text (Bosten, Barkol, Zhuyeze, Donggi Cona, and Luanhaizi Lakes), as well as the surrounding regions (Tibetan Plateau, Chinese Loess Plateau, Qaidam and Tarim Basins, and Gobi desert). Also showing the climatic systems impacting Lake Qinghai area including the East Asian and Indian summer monsoons (labeled by EASM and ISM, respectively), and the Westerly winds generalized as the mean locations of jet stream in January and July (Zhang and Lin, 1992). (b) Geographic configuration of the Lake Qinghai drainage basin and its major feeding rivers (after Jin et al., 2011). The sampling sites for sediment cores (1Fs, QH03-02, QH03-14, QH2000, QH07, and 14B), lake surface sediments, loess, and suspended river sediments along the major rivers are shown. Dashed lines show the boundary of the Lake Qinghai catchment.

GLAD800 drilling system (Fig. 1). The location of the drilling site was chosen based on the thickness and distribution of lake sediments by an intensive geophysical survey of Lake Qinghai, to ensure that the core is ideally located to monitor the lake conditions (An et al., 2006, 2012). Three lithologic units of the core are readily distinguished by grain size, %$CaCO_3$, and TOC (An et al., 2012). The uppermost 5.0 m is composed mainly of silty clay or clays with horizontal bedding and has high carbonates (40–60%) and TOC (averaging 4.6%). The lithology in the middle unit (5.0–9.0 m) shifts to gray and grayish-yellow silty clay with silt layers, with average contents of 24.3% $CaCO_3$ and 0.8% TOC. The lowest part (9.0–18.6 m) is dominated by silty clay, loess-like silt and fine sand layers, with roughly constant $CaCO_3$ and TOC contents at 17.3% and 0.3%, respectively (An et al., 2012).

The age model for the core 1Fs was based on accelerator mass spectrometry (AMS)-^{14}C dates of 52 bulk TOC, 6 *Ruppia maritima* seeds (from 4.16 to 4.97 m), and 7 plant remains samples (from 6.70 to 8.38 m) (An et al., 2012; Zhou et al., 2014). After comparing three approaches for these ^{14}C dates, Zhou et al. (2014) adopted the linear regressions in segments to construct the age model for the core 1Fs as shown in Fig. 2. The three units in 1Fs had different reservoir ages, possibly resulting from variable lithology and sedimentation rates. The average reservoir age was ~135 a for the uppermost 5.0 m. Assuming that there were no discontinuities in the core, the average reservoir ages in the middle unit (5.0–9.0 m) and the lowest part (9.0–18.6 m) were 1143 a and 2523 a, respectively. This age model suggested the oldest sediment from the core 1Fs to be 32 ka. The validity of the age model was supported by a good correlation of sedimentary proxy with the speleothem δ^{18}O record from a nearby region (An et al., 2012).

We also worked on two short cores, QH03-02 (36°40′47.5″N, 100°07′19.5″E, 28.5 cm long) and QH03-14 (37°00′59.9″N, 100°13′24.1″E, 27.0 cm long), collected from the southern and northern sub-basins, respectively (Fig. 1b). These two cores were dated using both ^{210}Pb and ^{137}Cs activities. The first ^{137}Cs activity (1952 AD) was detected at 6.50–6.75 cm depth in the core QH03-02, and at 7.00–7.25 cm depth in the core QH03-14. These agree well with the CRS models, yielding dates of 1951.6 AD for QH03-02 and 1953.2 AD for QH03-14, respectively (Jin et al., 2010a). Sediment samples from these two short cores since 1950s were used for leaching experiments.

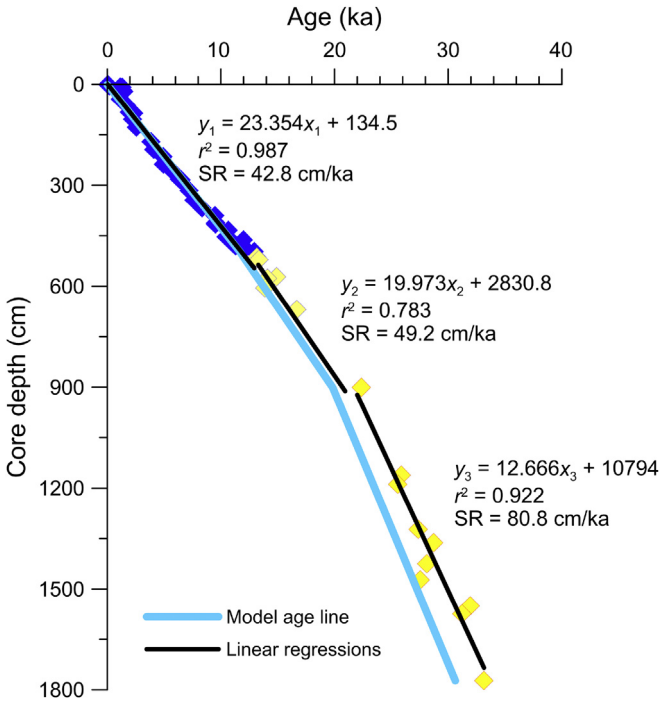

Fig. 2. The age model for core 1Fs using the linear regressions in segments after Zhou et al. (2014). The ^{14}C data are divided into three segments according to their respective lithology and sedimentation rates (SR). Also shown is SR for each unit calculated from the age model, along with regression equations.

3.3. Rb, Zr and Sr measurements

We have measured Rb, Zr, and Sr concentrations for all samples of lake and river sediment samples, 1Fs sediments at 1 cm intervals, and loess samples. These samples were firstly dried and were ground to a fine powder <38 μm in an agate mortar. About 5-g powder sample was then compacted into a disc with a diameter of 32 mm under 30 tonforces. Bulk sedimentary Rb, Zr and Sr concentrations in each sample were analyzed on an Axios advanced wavelength dispersive X-ray fluorescence spectrometer (WD-XRF; PANalytical, Ea Almelo, The Netherlands) at Institute of Earth Environment, Chinese Academy of Sciences (IEECAS). The measurements were calibrated using 26 certified reference materials including 15 soil samples (GSS 1–7 and 9–16) and 11 stream sediment samples (GSD 1–11). The relative standard deviation, based on repeated analyses of two standards (GSS-8, GSD-12), was less than 1 ppm for all elements.

3.4. HOAc-leachable elements

To estimate leachable Ca and Sr, 25 mL solution of 0.5 M acetic acid (pH = ~5) was used to leach 0.5 g most recent (since 1950s) lake sediments from the short cores QH03-02 and QH03-14. After leaching for 12 h in an ultrasonic bath under room temperature, supernatant of each sample was separated from residual by centrifuging at 500 rpm for 10 min. The contents of Ca and Sr in the supernatant were analyzed by a Leeman Labs Profile ICP-AES at the State Key Laboratory of Lake Sciences and Environment. The precision of these analyses was ~2% at the 95% confidence level.

4. Results and discussion

4.1. Surface sediment chemistry

Fig. 3a shows Rb/Sr versus Sr of surface sediments for Lake Qinghai, five major contributing rivers, and local loess. Lake surface sediments show highest Sr and thus lowest Rb/Sr ratio, whereas sediments from Hargai, Quanji and Shaliu rivers show lowest Sr and highest Rb/Sr; and local loess, Buha and Heima suspended river sediments display intermediate values in Sr and Rb/Sr. Because Sr has a much higher activity than relatively more inert behavior of Rb (e.g. Dasch, 1969; Chen et al., 1999; Jin et al., 2006), Rb and Sr are easily fractionated during weathering processes on the Earth's surface. Dominated by carbonate weathering within the Lake Qinghai catchment (Jin et al., 2011), both Ca and Sr are readily transported into Lake Qinghai in dissolved forms by rivers and can subsequently be removed via precipitation of authigenic carbonates (see Section 4.2). This process alone would lead to lacustrine precipitation to be characterized by lower Rb/Sr than loess and river depositions, as observed in surface sediments shown in Fig. 3a. The Rb/Sr contrast may also be enlarged by the fact that the latters are more depleted in Sr (Fig. 3a).

Similar to Rb and Sr behaviors, the contrasting geochemical properties of Ca and Zr cause Ca/Zr to behave in an opposite fashion to Rb/Sr: authigenic carbonate-enriched sediments have low-Rb/Sr

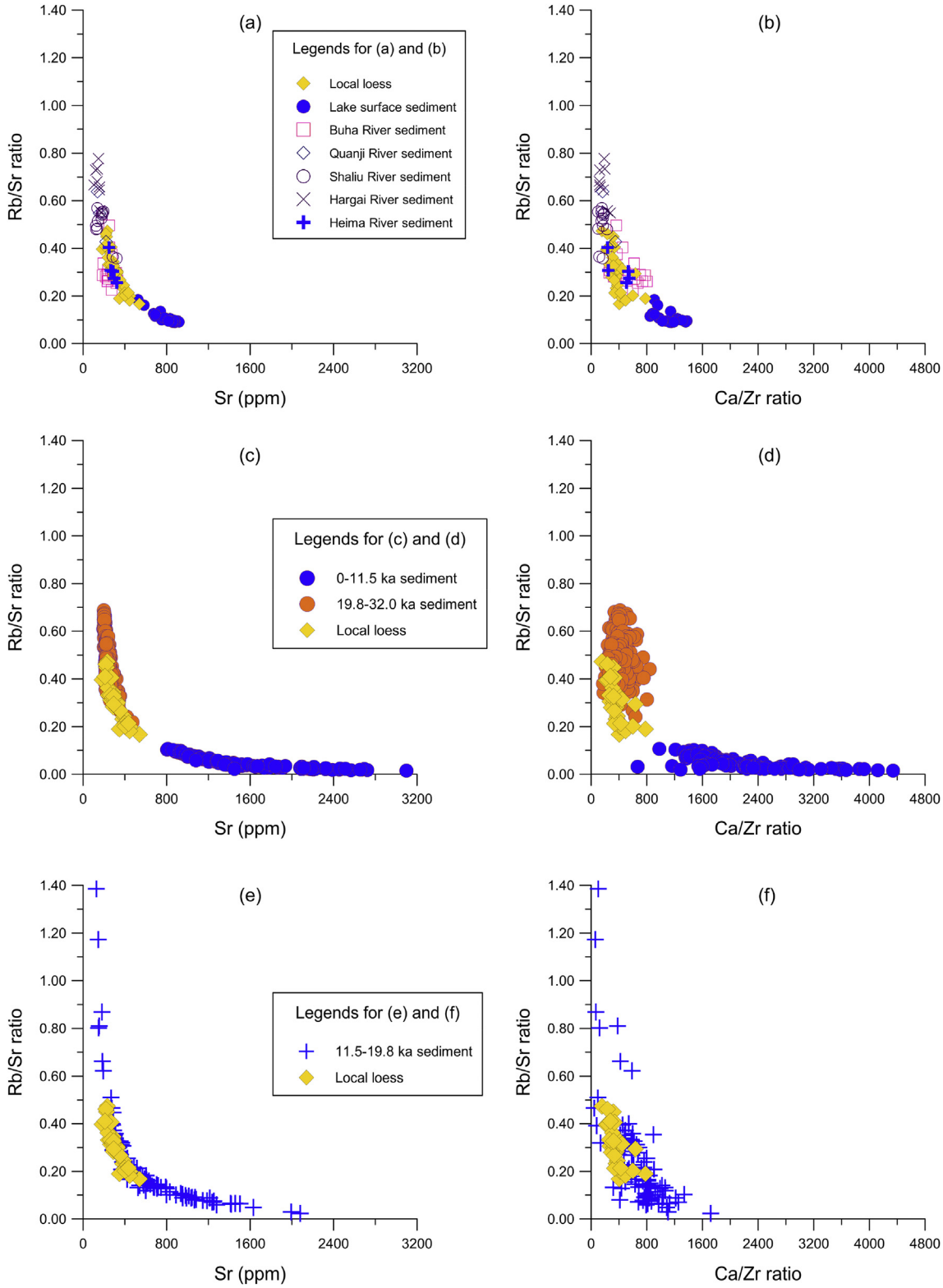

Fig. 3. Rb/Sr ratios vs. Sr concentrations and Ca/Zr ratios. For comparison, all panels plotted with the same scale on X and Y axis. (a, b) Modern lake and suspended river sediments within the Lake Qinghai catchment, (c, d) 0–11.5 ka and 19.8–32.0 ka 1Fs lake sediments, and (e, f) 11.5–19.8 ka 1Fs lake sediments, along with local loess for comparison.

and high-Ca/Zr, whereas sediments dominated by eolian dust would show high-Rb/Sr but low-Ca/Zr (Fig. 3b). Therefore, Rb/Sr and Ca/Zr are here employed to infer the fluxes of authigenic carbonates versus eolian dust into the lake.

4.2. Short core records and solute budget

Fig. 4 show leachable Ca and Sr contents of lake sediments for two short cores QH03-02 and QH03-14 during ~1950–2000 AD. Ca

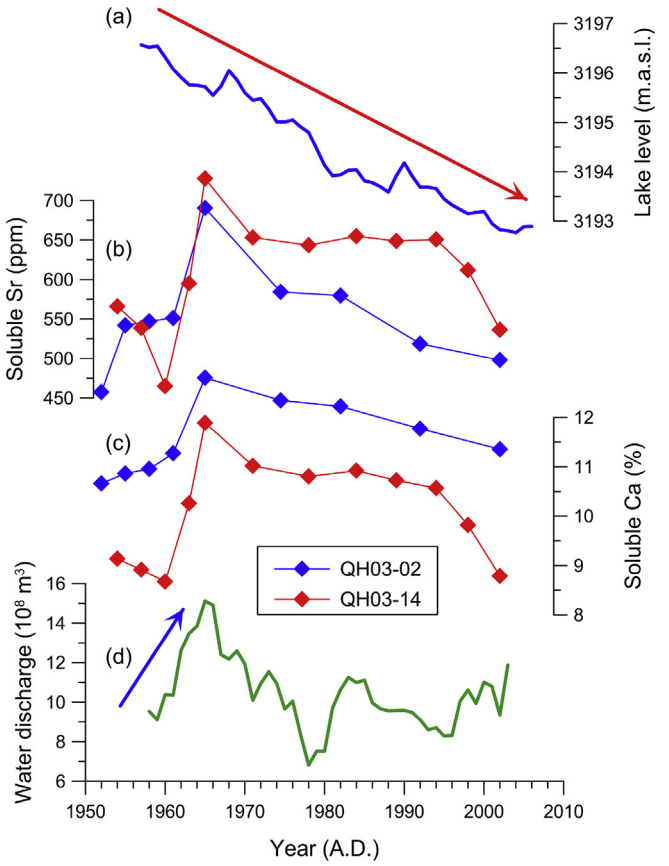

Fig. 4. Variations in lake level (a), soluble Sr (b) and Ca (c) concentrations of the lake sediments in Lake Qinghai, Buha River water discharge (d) during rainy season (late May to September) since 1950 A.D. Soluble Ca and Sr percentages of the lake sediments are from the cores of QH03-02 (southern sub-basin) and QH03-14 (northern sub-basins). The ages of both cores were well dated by ^{210}Pb and ^{137}Cs (Jin et al., 2010a). Blue and red arrows show trends in water discharge, lake water level, and soluble Ca and Sr concentrations. (For interpretation of the references to color in this figure legend, the reader is referred to the web version of this article.)

and Sr contents in both cores rose (by ~2% and ~200 ppm, respectively) from 1950 to 1968 AD, followed by a decline (by ~2% and ~170 ppm, respectively) from ~1968 to ~2000 AD (Fig. 4b and c). This pattern differs from the monotonic decrease of the lake level over the same time interval (Fig. 4a), suggesting that evaporation is not a major factor controlling Ca and Sr contents in lake sediments. By contrast, leachable Ca and Sr contents of lake sediments show a strong similarity with water discharge during rainy seasons (late May to September) since 1950 AD (Fig. 3d). This indicates a mechanistic link between Lake Qinghai sediment Ca and Sr contents and the regional rainfall, via authigenic carbonate precipitation in the lake.

There are a few factors influencing the development of huge Lake Qinghai into a brackish, Ca^{2+}-limited ecosystem. First, due to its location in a semiarid area, the evaporation in this region is 3–4 times greater than precipitation (Li et al., 2007), resulting in the enrichment of Na^+, Mg^{2+}, Cl^-, and HCO_3^- in lake water (Jin et al., 2010b). Second, under low rainfall (averaging 383 mm/a in 1959–2011) and low temperature (averaging 1.2 °C annually) conditions, dissolved loads into the lake are dominated by carbonate weathering of underlying limestone within the catchment (Jin et al., 2011). Third, lake water is supersaturated with respect to aragonite and calcite, resulting in a constant precipitation of authigenic carbonates (aragonite dominance) to the lake floor (Jin et al., 2010b, 2013). Under such a condition, calcium becomes the key-limiting element in Lake Qinghai, where any available Ca^{2+} (and Sr^{2+}) from rivers would be rapidly removed by precipitation of authigenic carbonates, resulting in very low Ca^{2+} and Sr^{2+} in the lake itself (Jin et al., 2010b). Consequently, Ca and Sr contents of lake sediments would be largely controlled by dissolved Ca^{2+} and Sr^{2+} fluxes carrying into the lake by runoff within the catchment, as indicated above (Fig. 4). This finding allows us to link lake sediment Ca and Sr contents to the regional rainfall intensity, and further to hydroclimate changes in the Lake Qinghai area. This linkage is employed to interpret the geochemical variations in sediments from the core 1Fs.

4.3. Rb, Sr, and Ca/Zr stratigraphy and depositional conditions since the last glacial

Fig. 5 shows sedimentary Rb, Sr, Rb/Sr, and Ca/Zr in Lake Qinghai core 1Fs during the past 32 ka. The records can be divided into three

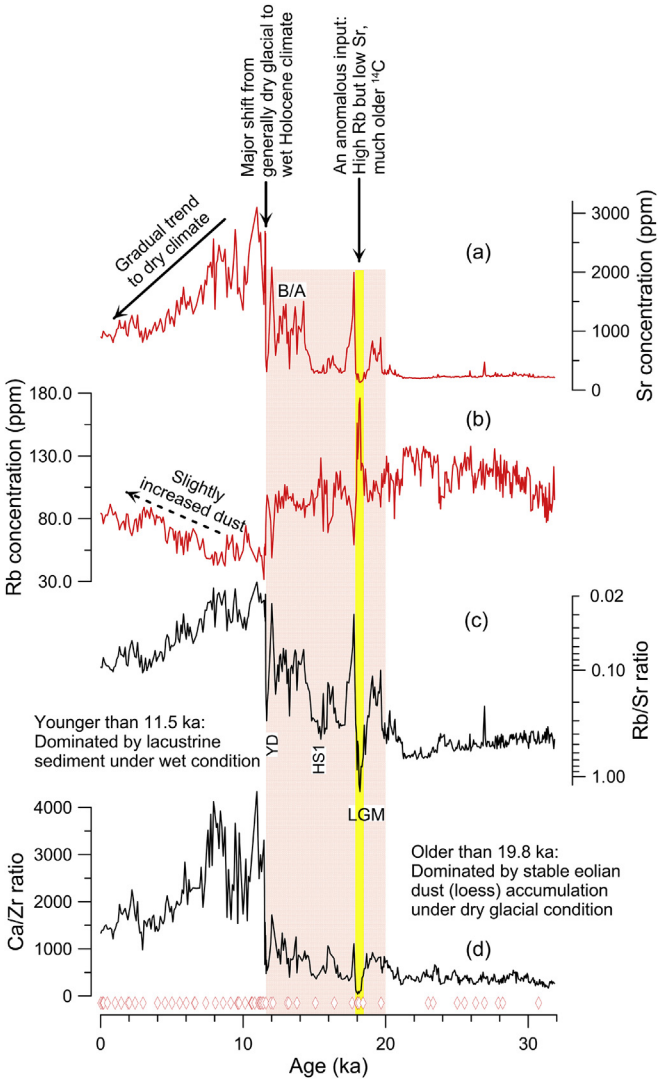

Fig. 5. Rb (a), Sr (b), Rb/Sr (c), and Ca/Zr (d) for core 1Fs from Lake Qinghai. Rb and Sr values are in ppm, and the scale of Rb/Sr is descending logarithm, with base 10. Orange and yellow shadings indicate the transitional and anomalous changes during the last deglacial and the LGM (Last Glacial Maximum) (see the text). YD = Younger Dryas, B/A = Bølling/Allerød, and HS1 = Heinrich Stadial 1. Red open diamonds at the bottom denote radiocarbon dates (An et al., 2012; Zhou et al., 2014). (For interpretation of the references to color in this figure legend, the reader is referred to the web version of this article.)

stages according to the trends and variability of Rb, Sr, Rb/Sr and Ca/Zr. From 32 to ~19.8 ka, Lake Qinghai sediment is characterized by constant low Sr but high Rb concentrations (Fig. 5a and b). Rb and Sr range from 77 to 138 ppm (averaging 115 ppm) and from 195 to 473 ppm (averaging 236 ppm), respectively. As a result, Rb/Sr ratios are high, ranging from 0.22 to 0.69 (Fig. 5c). In contrast, Ca/Zr ratios are constantly low, ranging from 172 to 841 with an average of 386 (Fig. 5d).

The relative stable compositions were interrupted by episodic precipitates with high-Sr, high-Ca/Zr, but low-Rb during the last deglacial (~19.8–11.5 ka), characterized by a frequent fluctuation in sedimentary geochemistry. Both Rb and Rb/Sr are relatively high throughout this period, in particular during the LGM, the Heinrich Stadial 1 (HS1) and the Younger Dryas (YD), but Sr and Ca/Zr also appear high during the periods of Bølling/Allerød (B/A) and following the LGM (Fig. 5). Notably, there is one additional distinct peak of Sr at ~12.0 ka within the YD event. In addition, there was an anomalous input during the LGM, marked by much higher Rb/Sr but lower Ca/Zr ratios (yellow shading, Fig. 5c and d).

A dramatic shift in sediment geochemistry occurs at ~11.5 ka. Rb and Rb/Sr drop from 90 to 32 ppm and from 0.24 to 0.02, respectively, whereas Sr and Ca/Zr shift from 377 to 2694 ppm and from 474 to 3302, respectively. During the Holocene, Lake Qinghai sediments are characterized by high Sr and %$CaCO_3$ but relatively low Rb concentrations. Rb and Sr range from 32 to 91 ppm (averaging 67 ppm) and from 805 to 3100 ppm (averaging 1492 ppm), respectively, resulting in lower Rb/Sr ratios of 0.01 to 0.11 (Fig. 5). In contrast, Ca/Zr ratios are high, ranging from 669 to 4339 with an average of 2086. Since ~8.0 ka, the sediments are marked by a gradual increase in Rb, but a reduction in both Sr and Ca/Zr.

The 1Fs Rb, Sr, Rb/Sr, and Ca/Zr records indicate that the sediment succession in Lake Qinghai has changed dramatically during the past 32 ka and was closely linked to climate-driven shifts in hydrology and dust deposition (Fig. 5). We have compared Rb/Sr versus Sr and Ca/Zr in core 1Fs with those of local loess samples (Fig. 3c–f). Fig. 3c and d shows that sediment Rb/Sr, Ca/Zr and Sr data during 32–19.8 ka overlap with those of local loess. During this time interval, silt and clay dominate the lake sediments (An et al., 2012), characterized by constantly low Sr and Ca/Zr but high Rb concentrations, indicating a stable source. These sediments are dominated by typical loess with high Rb/Sr but low Ca/Zr ratios. During this period, sediments have low and constant organic detritus (0.3%) and $CaCO_3$ (17.3%), high and varying coarse grains (An et al., 2012) (Fig. 6), and low primary productivity dominated by C_3 plants (Shang, 2009; Thomas et al., 2014). The grain-size distribution during this period is similar to that of loess from the catchment (An et al., 2012), resulting in a high sedimentation rate (an average of 80.8 cm/ka versus 42.8 cm/ka in the Holocene; Fig. 2). The sedimentation rate is close to that of silt-like loess (~1 mm/a) nearby the Bird Island onshore Lake Qinghai since the Little Ice age (Zhou et al., 2015). These together suggest that Lake Qinghai during 32–19.8 ka was likely to be a desiccated basin, and its sediments were dominated by eolian dust deposition under a dry glacial condition. Similarly, the Bosten Lake basin was covered by meters of eolian sand between the late glacial and 8.4 ka, followed by a layer of dark peat and then a stable lake since 8 ka (Wünnemann et al., 2006). The deposition of eolian sand was also attributed to dry climate conditions under a very low or even desiccated lake (Huang et al., 2009). The eolian-dominated environment around 32–18 ka was also inferred by pollen assemblage from two lacustrine-wetland sequences in the western part of the Chinese Loess Plateau (Feng et al., 2007; Wu et al., 2009). Under dry conditions, salt lake area in the western Qaidam Basin had extended at large scale around 31–26 ka (Zheng et al., 1989), and deserts in northern and northwestern China had expanded during 26–16 ka (Lu et al., 2013).

Between 19.8 and 11.5 ka, this loess deposition was interrupted by intervals with fluctuating Rb and Sr concentrations and Rb/Sr and Ca/Zr ratios (Fig. 5). We interpret low Rb/Sr but high Ca/Zr ratios to reflect lacustrine precipitates. Based on our short core records (Fig. 4, Section 4.2 above), the increased Ca and Sr may result from some riverine Ca^{2+} and Sr^{2+} input derived from the catchment weathering, supported by some sediments offsetting the loess endmember (Fig. 3e and f). Riverine Ca^{2+} and Sr^{2+} was present but not dominant during this deglaciation, indicating that the lake was occupied by shallow water during some periods, in particular during the entire B/A warming period. Riverine inputs also diluted Rb in the sediments (Fig. 5b). The lacustrine condition is further supported by intermittent appearance of ostracod shells (Lister et al., 1991; Liu et al., 2007) and their varying $\delta^{18}O$ ratios between 19.8 and 11.5 ka (Fig. 6c). Loess deposition was, however, apparently high throughout this period, notably during the LGM, the HS1 and the YD (Fig. 5). The timing of these events might have some potential uncertainties owing to the loadings of various sources. Notably, there was a perturbation within the YD event, characterized by two peaks in Rb/Sr ratios (Fig. 5c). In addition, there was an anomalous input during the LGM, marked by much older ^{14}C (a TOC peak, eight ^{14}C data 17,000–34,000 a older compared to adjacent samples that remain in chronostratigraphic order; Zhou et al., 2014), much higher Rb/Sr but lower Ca/Zr ratios (yellow shading in Fig. 5), and high TOC but low $CaCO_3$ (Fig. 6), which was interpreted to be an important hydrological event or the melting of frozen soil surrounding the lake (An et al., 2012; Zhou et al., 2014). These anomalies are important, because such an event could cause an unusually large reservoir effect and geochemical signals.

Since 11.5 ka, Lake Qinghai sediment is characterized by low Rb/Sr but high Ca/Zr ratios. Rb/Sr, Ca/Zr and Sr of samples from core 1Fs differ from those of loess samples and exhibit more similarity with surface lake sediments (Fig. 3c and d). We interpret these high Ca and Sr but low Rb (Figs. 5a and 6b) to be caused by a dominant lacustrine deposition in Lake Qinghai during the whole Holocene. This interpretation is supported by (1) high $CaCO_3$ and TOC contents (Fig. 6b, d) (Shen et al., 2005; An et al., 2012), (2) finer grain size (Fig. 6e) (An et al., 2012), and (3) consistent and negative $\delta^{18}O$ ratios of ostracod shells (Fig. 6c) (Lister et al., 1991; Liu et al., 2007; An et al., 2012). Moreover, the appearance of the authigenic aragonite (Fig. 6b) along with gray–green clay indicates a shift to a high runoff and rainfall; aragonite dominates $CaCO_3$ content. Since ~8.0 ka, the sediment is marked by a gradual increase in Rb, indicating a slightly gradual increase in dust input. These changes seem to be a result of a regional change in climate rather than hydrology alone, because there is a gradual decline in Sr and $CaCO_3$ contents, indicative of runoff and also rainfall.

4.4. Hydroclimatic determinants of sediment development

The overall trend of the 32 ka hydroclimate in Lake Qinghai reflected by the Rb/Sr and Ca/Zr records is characterized by a dry glacial, a highly variable deglacial, and a humid climate during the early Holocene, with a declining monsoon to the present, similar to previous records (e.g. Lister et al., 1991; Shen et al., 2005; An et al., 2012; Liu et al., 2003, 2014). The Rb/Sr and Ca/Zr records contain some processes and depositional conditions previously unobserved in Lake Qinghai, including dominated loess accumulation under dry glacial conditions, high-amplitude millennial scale fluctuation during the deglaciation, and a YD perturbation. These observations provide insights into high-elevation Lake Qinghai depositional conditions, hydroclimate variability, and forcing mechanisms.

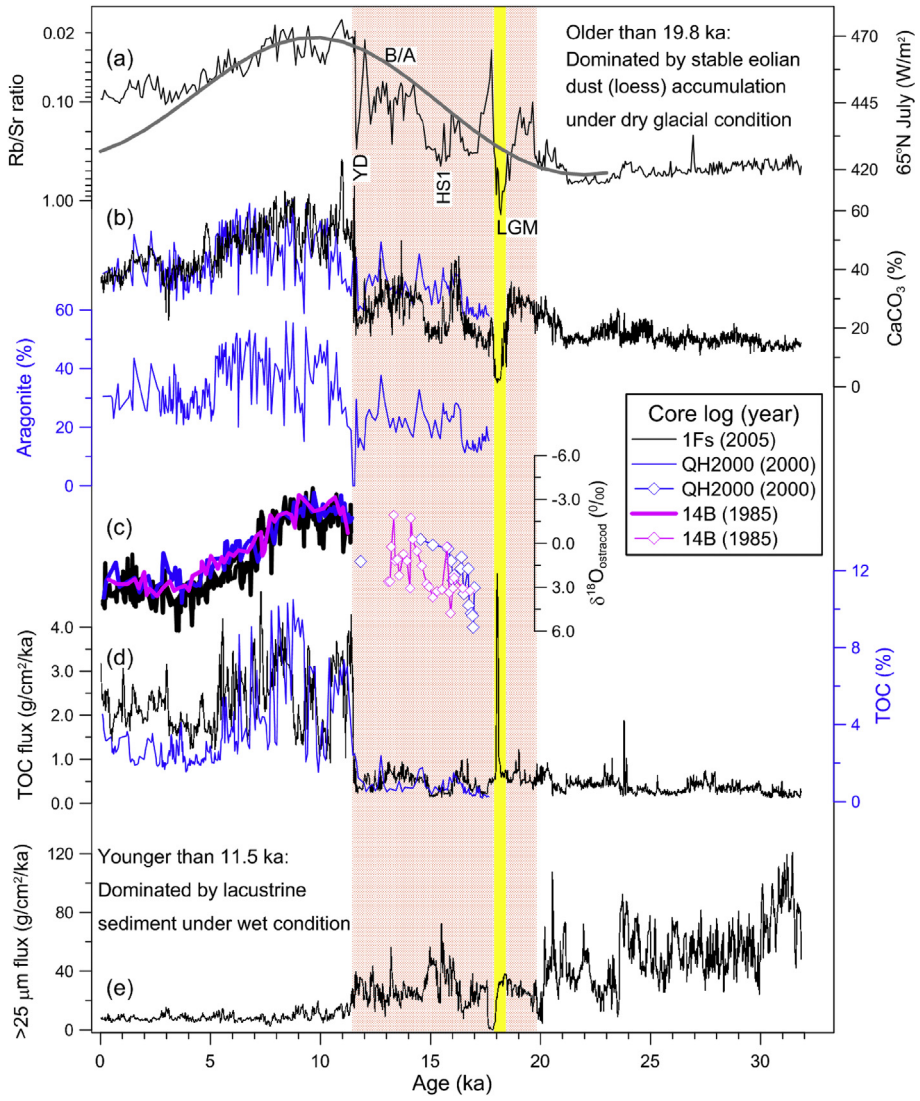

Fig. 6. Lake Qinghai Rb/Sr compared to other sedimentological and biological reconstructions. (a) 1Fs Rb/Sr ratios superimposed by the July insolation at 65°N (gray). July insolation is in watts per square meter. (b) Percent carbonate and aragonite for cores of 1Fs (black) (An et al., 2012) and QH2000 (blue) (Shen et al., 2005). (c) Lake Qinghai ostracod shell $\delta^{18}O$ ratios from cores of 14B (pink) (Lister et al., 1991), QH2000 (blue) (Liu et al., 2007), and 1Fs (black) (An et al., 2012). Being considered limited data before 11.5 ka, symbols are marked. (d) Total organic carbon (TOC) flux for core 1Fs (black) (An et al., 2012) and TOC content for core QH2000 (blue) (Shen et al., 2005). The abrupt increases at 11.5 ka in both records are likely due to a sedimentological shift as well as a precipitation increase. (e) Flux of coarse grains in Lake Qinghai sediment, with larger flux corresponding to strong westerly winds (An et al., 2012). Age models for cores 14B (Lister et al., 1991) and QH2000 (Shen et al., 2005; Liu et al., 2007) adjusted to match for core 1Fs based on the alignment of their TOC contents. Orange and yellow shadings and labeled climatic events are as same as Fig. 5. (For interpretation of the references to color in this figure legend, the reader is referred to the web version of this article.)

The desiccation during the last glacial to the early Holocene has been suggested by nearly all lake sediment drillings in the central Asia, such as Bosten, Barkol, and Zhuyeze Lakes (locations shown in Fig. 1a) (Ran and Feng, 2013; Cai et al., 2014). However, the timing of the transition from desiccation to lacustrine conditions differs spatially. As the largest inland freshwater lake in China, Bosten Lake remained desiccated until 8.4 ka (Huang et al., 2009). Likewise, a high-resolution fossil pollen record from sedimentary cores at Barkol Lake (eastern Xinjiang) indicates that the lake was dried up until 8.9 ka (Tao et al., 2010). Similar to Lake Qinghai, a shift to lacustrine precipitates in Zhuyeze and Donggi Cona Lakes occurred at the beginning of the Holocene (Long et al., 2010; Dietze et al., 2013). It appears that, during the last glacial period, all these lake basins largely served as dust sinks. The consistent distribution of high Rb but low Sr, Ca/Zr and TOC levels in Lake Qinghai sediments provides strong evidence for an eolian origin of sediment during the dry glacial periods. This prolonged dry period might have been caused by weak Asian monsoons (Chen et al., 2008; Ran and Feng, 2013; Cai et al., 2014), further supported by pollen preserved in sediments during the last glacial period (Shang, 2009). The pollen assemblage during that period in Lake Qinghai sediments is characterized by *Artemisia*, Chenopodiaceae, and *Ephedra*, indicatives to desert and grassland, but no aqueous pollen. By contrast, Northern Hemisphere westerly winds were strong during 32 and 20 ka (Sun et al., 2012), facilitating dust transportation to Lake Qinghai from the desert areas such as the Qaidam and Tarim Basins, and the Gobi desert (Fig. 1). The feasibility of long-distance transport of dust from the central Asia is supported by frequent dust storms during the springtime (Wan et al., 2012) and dissolved chemistry of seasonal river water within the Lake Qinghai catchment (Jin et al., 2011). The fluctuations of Rb and coarse grains during 19.8–11.5 ka (Figs. 4 and 6e) may suggest variations in westerly

winds (strength and locations) and/or dust sources during the dry glacial. The earlier onset of dominant lacustrine precipitates in Qinghai and Zhuyeze Lakes than in Bosten and Balkol Lakes, with potential dating uncertainties, could be attributed to gradual transgression northward in the early Holocene associated with increased summer insolation (e.g. Ran and Feng, 2013).

An intriguing feature of our reconstruction is frequent and large fluctuations in Rb, Sr, Rb/Sr and Ca/Zr ratios between 19.8 and 11.5 ka. These fluctuations indicate alternations between eolian and riverine inputs under unstable transitional conditions during the deglaciation. During this deglacial period, the lake did not desiccate completely (Thomas et al., 2014) and was occupied occasionally by shallow water, in particular, during the B/A warm period. Wet conditions during the B/A warm period were also recorded by other nearby lake sediments, such as in Lakes Luanhaizi and Donggi Cona (Herzschuh et al., 2010; Dietze et al., 2013; Wang et al., 2014). The alternations of wet and dry periods are also reflected by fluctuating TOC, grain size, %$CaCO_3$, and discontinuous preservation of ostracod shells (Fig. 6). Similarly, multi-proxy analysis (pollen, %$CaCO_3$, TOC and its $\delta^{13}C$) for the core QH2000 also recorded the frequently fluctuated climate and the B/A and YD climatic oscillations during the transitional period from the Late Glacial to the Holocene (Shen et al., 2005). Also using %$CaCO_3$ and TOC from the core QH07 of Lake Qinghai (Fig. 1b) as environmental indicators, however, stable, cold and arid environment during the entire LGM and late glacial time was inferred, with little or no evidence of a warm interval correlative with the B/A (Liu et al., 2014). These differences in the recognition of the climatic events can be attributed to sensitivities of various proxies and/or chronology uncertainties. These observations indicate that the Indian/Asian summer monsoon front began to reach the northeastern Tibetan Plateau until the early Holocene. Nevertheless, the records between 19.8 and 11.5 ka in Fig. 6 suggest that dust deposits dominated in particular during the LGM, the HS1 and the YD, possibly linked to prevailing westerly winds over the monsoons. These fluctuations occurred more frequently than would be expected from orbital forcing alone, probably indicating a nonlinear amplification of hydroclimatic variability on high-elevation Lake Qinghai relative to low elevations (Liu et al., 2009; Diffenbaugh et al., 2012). One distinct peak of both Sr (Rb/Sr) and aragonite at 12 ka during the YD provides a best example of a superimposion of a wet period upon millennial-scale dry events. Therefore, the nonlinear changes in sedimentary geochemistry attest that sedimentary geochemical properties respond sensitively to not only sediment sources but also hydrological conditions associated with the regional climate changes.

The abrupt shift to a humid climate at ~11.5 ka in the Lake Qinghai region was responsible for large increases in TOC, aragonite, and %$CaCO_3$ (Fig. 6), as well as significant growth of C_4 plants (Thomas et al., 2014). The abrupt transition between the late Pleistocene and the Holocene was also inferred from the cores QH2000 and QH07, though the time for the transition was placed at 10.8 ka (Shen et al., 2005) or at around 11.5 ka (Liu et al., 2014). These indicate a dramatic increase in lake water and the formation of a deep lake since the onset of the Holocene. The peak values during ~11.5–8.0 ka shown in Fig. 6 indicate the highest lake level during the early Holocene and the most humid conditions over the last 32 ka. Similarly, the warmest and wettest was indicated to occur at the early Holocene, but the persist times differed from 6.5 ka (Shen et al., 2005) or ~9.0 ka (Liu et al., 2014). At the neighboring Lake Gonggi Cona, its initial lake-level rose also at ~11 ka, reached its maximum ~9.2 ka and fell at ~8.5 ka (Dietze et al., 2013). The high lake levels may be attributed to an enhanced summer precipitation triggered by orbital forcing of Indian/Asian monsoonal climate (e.g. Dietze et al., 2013; Ran and Feng, 2013; Wang et al., 2014), and/or by maximum summer insolation contrast between 30°N and 15°N (Liu et al., 2014). The humid climate would have favored carbonate weathering within the catchment whose underlying bedrocks are dominated by the late Paleozoic marine limestone. The increased carbonate weathering would raise Ca^{2+} and Sr^{2+} supplies to the lake through runoff. Analogue to the most recent conditions (Fig. 4, Section 4.2 above), this riverine Ca^{2+} and Sr^{2+} input would be directly precipitated to the lake floor in the form of carbonate minerals. Indeed, modern sediment trap studies show dominant authigenic origin of aragonite and calcite (Jin et al., 2013), and carbonates during the whole Holocene mainly consist of authigenic aragonite in core QH2000 (Fig. 6b) (Liu et al., 2003). Meanwhile, wetter and warmer conditions were also favorable for primary production, as indicated by increased TOC flux and continuous preservation of ostracod shells (Fig. 6c and d). Furthermore, high lake levels during the early Holocene inferred from low Rb/Sr and high Ca/Zr are consistent with negative $\delta^{18}O$ ratios of ostracod shells (Fig. 6c) (Lister et al., 1991; Liu et al., 2007; An et al., 2012).

The gradual reduction in Sr, %$CaCO_3$, and Ca/Zr ratios since ~8.0 ka tracks a decreasing rainfall associated with the decline in boreal summer insolation (Fig. 6a). In contrast to the last deglacial transition, Rb/Sr ratios in core 1Fs show less variability and almost linearly follow the 65°N summer insolation (Fig. 6a). Although there is a slightly gradual increase in dust input marked by Rb variation after ~8.0 ka, the synchronicity gives us confidence that there has been a deep permanent lake toward the present. The declining Sr, aragonite and %$CaCO_3$ in lacustrine sediments since the mid-Holocene point to a decline of rainfall, which, by making the region more arid, would enhance dust input to the lake. This is further confirmed by the continuous preservation of ostracod shells with positive $\delta^{18}O$ ratios (Fig. 6c; Liu et al., 2007; An et al., 2012) and by the gradual decline in TOC flux of the lake sediments (Fig. 6d). Similar reduction in monsoon precipitation since the mid-Holocene was also inferred from decreased %$CaCO_3$ and TOC in the core QH2000 and QH07 (Liu et al., 2003, 2014; Shen et al., 2005). The increasingly arid conditions and the decline in rainfall in the late Holocene were widely detected by most lacustrine and peat records along the transitional zone of the Asian summer monsoons (see a review in Cai et al., 2014). It is also consistent with monsoon-proxy records from elsewhere (e.g. Haug et al., 2001; Wang et al., 2005). These consistent findings support a tight link between subtropical hydroclimate and orbital forcing.

We interpret the increasing Rb/Sr during the middle and late Holocene to reflect declining rainfall and subsequently declining Lake Qinghai water levels. This would further suggest decreasing rainfall predominantly driven by weakening Indian/Asian summer monsoons that might have been linearly responding to the summer insolation. This clearly differs from the nonlinear responses of sedimentary geochemistry to the summer insolation during the last deglaciation, possibly because of different origins of sediment during the last deglacial (largely dust depositions under dry conditions) and the Holocene (lacustrine deposition under high lake levels). Only when sediments are lacustrine in origin, can its properties document the dynamics of lake hydrology in this region.

5. Conclusions

In this study, we present sedimentary Rb, Sr, Rb/Sr, and Ca/Zr results for surface sediments and downcores for Lake Qinghai. Measurements of surface sediments show that lacustrine sediments are characterized by high Sr, high Ca/Zr, and low Rb/Sr values, whereas loess and major river depositions have low Sr, low Ca/Zr, high Rb and Rb/Sr. Lacustrine Ca and Sr contents are mainly controlled by runoff, not by evaporation in Lake Qinghai, because nearly all dissolved Ca^{2+} and Sr^{2+} along with runoff would be

incorporated into authigenic carbonates under Ca^{2+}-limited, supersaturated lake water conditions.

Downcore Rb, Sr, Rb/Sr and Ca/Zr variability at the glacial-interglacial time scale mainly responds to changes in sediment sources and lake hydrology. Along with coarse grain size, low Ca/Zr, low TOC, desert and grassland pollen, and lack of ostracod preservation, the consistent distributions of high Rb and low Sr of glacial sediments (~32–19.8 ka), provide strong evidence that Lake Qinghai likely served as a dust sink during the last glacial period. The small variations of Rb, Sr and Ca/Zr of glacial sediments may be due to stable contributions of dust from various sources. During the last deglacial (~19.8–11.5 ka), the conditions of Lake Qinghai alternated between a dust sink and a shallow lake, with abrupt sedimentary changes in response to local hydrological changes during the HS1, the B/A, and the YD. A major shift to humid climate occurred at 11.5 ka, marking the onset of Lake Qinghai as a permanent lake throughout the Holocene. The rising sedimentary Rb/Sr ratios since the mid-Holocene are consistent with the declining runoff and lake level, which may be linked to the gradual weakening of Asian summer monsoons possibly due to a linear response to the 65°N insolation. Gradual weakening monsoons caused a slight increase in dust input during the late Holocene.

Our high-resolution 32-ka records for Lake Qinghai highlight (1) the importance of wind-blown dust and authigenic aragonite for sediment development and geochemistry, (2) the sensitive response of sediment geochemistry to the hydroclimatic changes since the last glacial in the northeastern Tibetan Plateau, and (3) a dramatic hydroclimatic shift at the transition of the last deglacial and the Holocene. This work offers an approach to investigate the sources of lake sediments and the use of sediment geochemical properties to infer the past lake status.

Acknowledgments

This work was supported by National Basic Research Program of China (2013CB956402), NSFC through grant 41225015 and by the CAS/SAFEA International Partnership Program for Creative Research Teams (KZZD-EW-TZ-03), ARC DP140101393 and FT140100993. We thank International Continental Drilling Program (ICDP) and the Chinese Environmental Scientific Drilling (CESD) Program for providing the cores and samples and chronology data. We especially thank Wu Feng and Wang Ping in the IEECAS for their kind help and suggestions for sample analyses and laboratory works. Thanks are extended to Yuewei Shi and Xinning Qiu at the Buha River Hydrological Station for their assistance with sample collection. Two anonymous referees are thanked for their insightful comments that improved the manuscript.

References

An, Z.S., Colman, S.M., Zhou, W.J., Li, X.Q., Brown, E.T., Jull, A.J.T., Cai, Y.J., Huang, Y.S., Lu, X.F., Chang, H., Song, Y.G., Sun, Y.B., Xu, H., Liu, W.G., Jin, Z.D., Liu, X.D., Cheng, P., Liu, Y., Ai, L., Li, X.Z., Liu, X.J., Yan, L.B., Shi, Z.G., Wang, X.L., Wu, F., Qiang, X.K., Dong, J.B., Lu, F.Y., Xu, X.W., 2012. Interplay between the Westerlies and Asian monsoon recorded in Lake Qinghai sediments since 32 ka. Sci. Rep. 2, 619. http://dx.doi.org/10.1038/srep00619.

An, Z.S., Wang, P., Shen, J., Zhang, Y., Zhang, P., Wang, S., Li, X., Sun, Q., Song, Y., Ai, L., Zhang, Y., Jiang, S., Liu, X., Wang, Y., 2006. Geophysical survey on the tectonic and sediment distribution of Qinghai Lake basin. Sci. China (Ser. D Earth Sci.) 49, 851–861.

Andreae, M.O., 1996. Raising dust in the greenhouse. Nature 380, 389–390.

Cai, Y.J., Jin, Z.D., Zhou, W.J., Liu, Y., Liu, Z., Li, B., Yu, X., Tan, L., Tian, L., Peng, Z., Song, S., Zhao, H., Lu, F., Hou, Y., An, Z., 2014. Asian monsoon variability recorded in other archives. In: An, Z.S. (Ed.), Late Cenozoic Climate Change in Asia, Developments in Paleoenvironmental Research, vol. 16. Springer Science Business Media Dordrecht. http://dx.doi.org/10.1007/978-94-007-7817-7_3.

Chen, J., An, Z.S., Head, J., 1999. Variation of Rb/Sr ratios in the loess-paleosol sequences of Central China during the last 130,000 years and their implications for monsoon paleoclimatology. Quat. Res. 51, 215–219.

Chen, K.Z., Bowler, J.M., Kelts, K., 1990. Paleoclimatic evolution within the Qinghai–Xizang (Tibet) Plateau in the last 40,000 years. Quat. Sci. 1, 21–31 (in Chinese).

Chen, F.H., Yu, Z.C., Yang, M.L., Ito, E., Wang, S., Madsen, D.B., Huang, X., Zhao, Y., Sato, T., Birks, H.J.B., Boomer, I., Chen, J., An, C., Wünnemann, B., 2008. Holocene moisture evolution in arid central Asia and its out-of-phase relationship with Asian monsoon history. Quat. Sci. Rev. 27, 351–364.

Colman, S.M., Yu, S.Y., An, Z.S., Shen, J., Henderson, A.C.G., 2007. Late Cenozoic climate changes in China's western interior: a review of research on Lake Qinghai and comparison with other records. Quat. Sci. Rev. 26, 2281–2300.

Dasch, E.J., 1969. Strontium isotopes in weathering profiles, deep-sea sediments, and sedimentary rocks. Geochim. Cosmochim. Acta 33, 1521–1552.

Dean, W.E., 1997. Rates, timing, and cyclicity of Holocene eolian activity in north-central United States: evidence from varved lake sediments. Geology 25, 331–334.

Dietze, E., Wünnemann, B., Hartmann, K., Diekmann, B., Jin, H., Stauch, G., Yang, S., Lehmkuhl, F., 2013. Early to mid-Holocene lake high-stand sediments at Lake Gonggi Cona, Northeastern Tibetan Plateau, China. Quat. Res. 79, 325–336.

Diffenbaugh, N.S., Scherer, M., Ashfaq, M., 2012. Response of snow-dependent hydrologic extremes to continued global warming. Nat. Clim. Change 3, 379–384.

Feng, Z.D., Tang, L.Y., Ma, Y.Z., Zhai, Z., Wu, H.N., Li, F., Zou, S., Yang, Q., Wang, W., Derbyshire, E., Liu, K.B., 2007. Vegetation variations and associated environmental changes during marine isotope stage 3 in the western part of the Chinese Loess Plateau. Palaeogeogr. Palaeoclimatol. Palaeoecol. 246, 278–291.

Fu, C.F., An, Z.S., Qiang, X., Bloemendal, J., Song, Y., Chang, H., 2013. Magnetostratigraphic determination of the age of ancient Lake Qinghai, and record of the East Asian monsoon since 4.63 Ma. Geology 41, 875–878.

Ganor, E., Foner, H.A., Gravenhorst, G., 2003. The amount and nature of the dustfall on Lake Kinneret (the Sea of Galilee), Israel: flux and fractionation. Atmos. Environ. 37, 4301–4315.

Guerzoni, S., Chester, R., Dulac, F., Herut, B., Loye-Pilot, M., Measures, C., Migon, C., Molinaroli, E., Moulin, C., Rossini, P., Saydam, C., Soudine, A., Ziveri, P., 1999. The role of atmospheric deposition in the biogeochemistry of the Mediterranean Sea. Prog. Oceanogr. 44, 147–190.

Haug, G.H., Hughen, K.A., Sigman, D.M., Peterson, L.C., Röhl, U., 2001. Southward migration of the intertropical convergence zone through the Holocene. Science 293, 1304–1308.

Henderson, A.C.G., Holmes, J.A., 2009. Palaeolimnological evidence for environmental change over the past millennium from Lake Qinghai sediments: a review and future research prospective. Quat. Int. 194, 134–147.

Herzschuh, U., Birks, H.J.B., Mischke, S., Zhang, C., Böhner, J., 2010. A modern pollen–climate calibration set based on lake sediments from the Tibetan Plateau and its application to a Late Quaternary pollen record from the Qilian Mountains. J. Biogeogr. 37, 752–766.

Huang, X.Z., Chen, F.H., Fan, Y.X., Yang, M.L., 2009. Dry late-glacial and early Holocene climate in arid central Asia indicated by lithological and palynological evidence from Bosten Lake, China. Quat. Int. 194, 19–27.

Ji, J.F., Shen, J., Balsam, W., Chen, J., Liu, L.W., Liu, X.Q., 2005. Asian monsoon oscillations in the northeastern Qinghai–Tibet Plateau since the Late Glacial as interpreted from visible reflectance of Qinghai Lake sediments. Earth Planet. Sci. Lett. 233, 61–70.

Jin, Z.D., Cao, J.J., Wu, J.L., Wang, S.M., 2006. A Rb/Sr record of catchment weathering response to Holocene climate change in Inner Mongolia. Earth Surf. Process. Landforms. 31, 285–291.

Jin, Z.D., You, C.F., Yu, J.M., 2009. Toward a geochemical mass balance of major elements in Lake Qinghai, NE Tibetan Plateau: a significant role of atmospheric deposition. Appl. Geochem. 24, 1901–1907.

Jin, Z.D., Han, Y.M., Chen, L., 2010a. Past atmospheric Pb deposition in Lake Qinghai, northeastern Tibetan Plateau. J. Paleolimnol. 43, 551–563.

Jin, Z.D., You, C.F., Wang, Y., Shi, Y.W., 2010b. Hydrological and solute budgets of Lake Qinghai, the largest lake on the Tibetan Plateau. Quat. Int. 218, 151–156.

Jin, Z.D., You, C.F., Yu, J.M., Wu, L.L., Zhang, F., Liu, H.C., 2011. Seasonal contributions of catchment weathering and eolian dust to river water chemistry, northeastern Tibetan Plateau: chemical and Sr isotopic constraints. J. Geophys. Res. Earth Surf. 116, F04006. http://dx.doi.org/10.1029/2011JF002002.

Jin, Z.D., Zhang, F., Li, F.C., Chen, L.M., Xiao, J., He, M.Y., 2013. Seasonal and interannual variations of the lake water parameters and particle flux in Lake Qinghai: a time-series sediment trap study. J. Earth Environ. 4, 1307–1314 (in Chinese with English abstract).

Kelts, K.R., Chen, K.Z., Lister, G.S., Yu, J.Q., Gao, Z.H., Niessen, N., Bonani, G., 1989. Geological fingerprints of climate history: a cooperative study of Qinghai Lake, China. Eclogae Geol. Helv. 82, 167–182.

Lawrence, C.R., Neff, J.C., 2009. The contemporary physical and chemical flux of aeolian dust: a synthesis of direct measurements of dust deposition. Chem. Geol. 267, 46–63.

Li, X.Y., Xu, H.Y., Sun, Y.L., Zhang, D.S., Yang, Z.P., 2007. Lake-level change and water balance analysis at Lake Qinghai, west China during recent decades. Water Resour. Manage. 21, 1505–1516.

LIGCAS (Lanzhou Institute of Geology of Chinese Academy of Sciences), 1979. A Synthetically Investigation Report on Qinghai Lake. Science Press, Beijing, pp. 1–23 (in Chinese).

Lister, G.S., Kelts, K.R., Chen, K.Z., Yu, J.Q., Niessen, F., 1991. Lake Qinghai, China: closed-basin lake levels and the oxygen isotope record for ostracoda since the latest Pleistocene. Palaeogeogr. Palaeoclimatol. Palaeoecol. 84, 141–162.

Liu, X.D., Cheng, Z.G., Yan, L.B., Yin, Z.Y., 2009. Elevation dependency of recent and future minimum surface air temperature trends in the Tibetan Plateau and its surroundings. Glob. Planet. Change 68, 164–174.
Liu, X.J., Colman, S.M., Brown, E.T., Henderson, A.C.G., Werne, J.P., Holmes, J.A., 2014. Abrupt deglaciation on the northeastern Tibetan Plateau: evidence from Lake Qinghai. J. Paleolimnol. 51, 223–240.
Liu, Z., Liu, D., Huang, J., Vaughan, M., Uno, I., Sugimoto, N., Kittaka, C., Trepte, C., Wang, Z., Hostetler, C., Winker, D., 2008. Airborne dust distributions over the Tibetan Plateau and surrounding areas derived from the first year of CALIPSO lidar observations. Atmos. Chem. Phys. 8, 5045–5060.
Liu, X.Q., Shen, J., Wang, S., Zhang, E., Cai, T., 2003. A 16000-year paleoclimatic record derived from authigenetic carbonate of lacustrine sediment in Qinghai Lake. Geol. J. China Univ. 9, 38–46 (in Chinese with English abstract).
Liu, X.Q., Shen, J., Wang, S., Wang, Y.B., Liu, W.G., 2007. Southwest monsoon changes indicated by oxygen isotope of ostracode shells from sediments in Qinghai Lake since the late Glacial. Chin. Sci. Bull. 52, 539–544.
Long, H., Lai, Z.P., Wang, N.A., Li, Y., 2010. Holocene climate variations from Zhuyeze terminal lake records in East Asian monsoon margin in arid northern China. Quat. Res. 74, 46–56.
Lu, H.Y., Yi, S., Xu, Z., Zhou, Y., Zen, L., Zhu, F., Feng, H., Dong, L., Zhuo, H., Yu, K., Mason, J., Wang, X., Chen, Y., Lu, Q., Wu, B., Dong, Z., Qu, J., Wang, X., Guo, Z., 2013. Chinese deserts and sand fields in Last Glacial Maximum and Holocene Optimum. Chin. Sci. Bull. 58, 2775–2783.
Mulitza, S., Heslop, D., Pittauerova, D., Fischer, H.W., Meyer, I., Stuut, J.B., Zabel, M., Mollenhauer, G., Collins, J.A., Kuhnert, H., Schulz, M., 2010. Increase in African dust flux at the onset of commercial agriculture in the Sahel region. Nature 466, 226–228.
Ran, M., Feng, Z., 2013. Holocene moisture variations across China and driving mechanisms: a synthesis of climatic records. Quat. Int. 313–314, 179–193.
Shang, X., 2009. Vegetation History and Climate Change in Lake Qinghai for the Last 34 cal ka BP. University of Chinese Academy of Sciences, pp. 46–71 (PhD thesis).
Shen, J., Liu, X.Q., Wang, S.M., Matsumotob, R., 2005. Palaeoclimatic changes in the Qinghai Lake area during the last 18,000 years. Quat. Int. 136, 131–140.
Sun, Y.B., Clemens, S.C., Morrill, C., Lin, X., Wang, X., An, Z.S., 2012. Influence of Atlantic meridional overturning circulation on the East Asian winter monsoon. Nat. Geosci. 5, 46–49.
Tao, S.C., An, C.B., Chen, F.H., Tang, L., Wang, Z., Lü, Y., Li, Z.F., Zheng, T., Zhao, J., 2010. Pollen-inferred vegetation and environmental changes since 16.7 ka BP at Balikun Lake, Xinjiang. Chin. Sci. Bull. 55, 2449–2457.
Thomas, E.K., Huang, Y., Morrill, C., Zhao, J., Wegener, P., Clemens, S.C., Colman, S.M., Gao, L., 2014. Abundant C_4 plants on the Tibetan Plateau during the Lateglacial and early Holocene. Quat. Sci. Rev. 87, 24–33.
Wan, D.J., Jin, Z.D., Wang, Y.X., 2012. Geochemistry of eolian dust and its elemental contribution to Lake Qinghai sediment. Appl. Geochem. 27, 1546–1555.
Wang, Y.J., Cheng, H., Edwards, R.L., He, Y., Kong, X., An, Z.S., Wu, J., Kelly, M.J., Dykoski, C.A., Li, X.D., 2005. The Holocene Asian monsoon: links to solar changes and north Atlantic climate. Science 308, 854–857.
Wang, Y., Herzschuh, U., Shumilovskikh, L.S., Mischke, S., Birks, H.J.B., Wischnewski, J., Böhner, J., Schlütz, F., Lehmkuhl, F., Diekmann, B., Wünnemann, B., Zhang, C., 2014. Quantitative reconstruction of precipitation changes on the NE Tibetan Plateau since the Last Glacial Maximum – extending the concept of pollen source area to pollen-based climate reconstructions from large lakes. Clim. Past 10, 21–39.
Wu, H., Ma, Y., Feng, Z., Sun, A., Zhang, C., Kuang, J., 2009. A high-resolution record of vegetation and environmental variations through the past ~25,000 yr BP in the western part of the Chinese Loess Plateau. Palaeogeogr. Palaeoclimatol. Palaeoecol. 273, 191–199.
Wünnemann, B., Mischke, S., Chen, F.H., 2006. A Holocene sedimentary record from Bosten Lake, China. Palaeogeogr. Palaeoclimatol. Palaeoecol. 234, 223–238.
Yan, J.P., Hinderer, M., Einsele, G., 2002. Geochemical evolution of closed-basin lakes, general model and application to Lakes Qinghai and Turkana. Sediment. Geol. 148, 105–122.
Zhang, J.C., Lin, Z.G., 1992. Climate of China. Wiley, New York, 376 pp.
Zheng, M.P., Xiang, J., Wie, X.J., 1989. The Salt Lakes in Qinghai-Tibet Plateau (in Chinese). Science & Technology Press, Beijing.
Zhou, W.J., Cheng, P., Jull, A.J.T., Lu, X., An, Z., Wang, H., Zhu, Y., Wu, Z., 2014. ^{14}C chronostratigraphy for Qinghai Lake in China. Radiocarbon 56, 143–155.
Zhou, L., Jin, Z.D., Wang, C.-H., Li, F., Wang, Y., Wang, X., Zhang, F., Chen, L., Du, J., 2015. Otolith microchemistry of modern versus well-dated ancient naked carp *Gymnocypris przewalskii*: implication for water evolution of Lake Qinghai. J. Asian Earth Sci. http://dx.doi.org/10.1016/j.jseaes.2015.02.006.